Andreas Flütsch[a,b], Thilo Schroeder[a,c], Jonas Barandun[a,d], Rafael Ackermann, Martin Bühlmann and Markus G. Grütter*

Specific targeting of human caspases using designed ankyrin repeat proteins

Abstract: Caspases play important roles in cell death, differentiation, and proliferation. Due to their high homology, especially of the active site, specific targeting of a particular caspase using substrate analogues is very difficult. Although commercially available small molecules based on peptides are lacking high specificity due to overlapping cleavage motives between different caspases, they are often used as specific tools. We have selected designed ankyrin repeat proteins (DARPins) against human caspases 1–9 and identified high-affinity binders for the targeted caspases, except for caspase 4. Besides previously reported caspase-specific DARPins, we generated novel DARPins (D1.73, D5.15, D6.11, D8.1, D8.4, and D9.2) and confirmed specificity for caspases 1, 5, 6, and 8 using a subset of caspase family members. In addition, we solved the crystal structure of caspase 8 in complex with DARPin D8.4. This binder interacts with non-conserved residues on the large subunit, thereby explaining its specificity. Structural analysis of this and other previously published crystal structures of caspase/DARPin complexes depicts two general binding areas either involving active site forming loops or a surface area laterally at the large subunit of the enzyme. Both surface areas involve non-conserved surface residues of caspases.

Keywords: apoptosis; cell death; DARPins; specific caspase targeting; X-ray crystallography.

[a]These authors contributed equally to this work.
[b]Present address: University of California, San Diego, 9500 Gilman Drive, La Jolla, CA 92093-0629, USA.
[c]Present address: Nextech Invest Ltd., Scheuchzerstrasse 35, 8006 Zurich, Switzerland.
[d]Present address: The Rockefeller University, Laboratory of Protein and Nucleic Acid Chemistry, 1230 York Avenue, New York, NY 10065, USA.
*Corresponding author: Markus G. Grütter, Department of Biochemistry, University of Zurich, Winterthurerstrasse 190, CH-8057 Zurich, Switzerland, e-mail: gruetter@bioc.uzh.ch
Andreas Flütsch, Thilo Schroeder, Jonas Barandun, Rafael Ackermann and Martin Bühlmann: Department of Biochemistry, University of Zurich, Winterthurerstrasse 190, CH-8057 Zurich, Switzerland

Introduction

A well-ordered removal of aberrant cells is important in multicellular animals to ensure the organism's cellular integrity. Thus, a variety of cell death pathways exist of which apoptosis is presumably one of the best-studied mechanisms, removing cells in an non-inflammatory manner thereby preventing a severe immune response in the organism (Taylor et al., 2008). Further, apoptosis plays a crucial role in embryonic development and tissue homeostasis. Although it is a highly controlled mechanism, its misregulation has been associated with severe diseases such as cancer or Alzheimer's disease (Rohn, 2010; Favaloro et al., 2012).

Proteases of the caspase family have been identified to be the major contributors of apoptosis. Caspases either induce (caspases 2, 8, 9, and 10) or execute (caspases 3, 6, and 7) the apoptotic signaling (Grütter, 2000). Furthermore, caspases 1, 4, 5, and 12 have been related to inflammatory pathways. Because all caspases share a high sequence and structural homology, specific targeting of one particular family member is limited with the contemporary available tools. The small peptide substrates or inhibitors lack specificity due to targeting of the highly conserved active site (McStay et al., 2008). Another more promising approach is the development of small molecule compounds that bind and inhibit caspases 3 and 7 outside the active site pocket, although the identified binding site for these compounds is conserved between both caspases (Hardy et al., 2004).

To increase a compound's specificity for a particular caspase, we used engineered binding proteins that provide larger binding interfaces and potentially also involve nonconserved residues. For our studies, we selected binders using a designed ankyrin repeat protein (DARPin) library. DARPins were designed based on repeat modules occurring in natural ankyrin proteins and consist of an N-terminal capping repeat (N-cap) followed by two (=NI2C) or three (=NI3C) internal and a C-terminal repeat (C-cap) (Binz et al., 2004). Each internal repeat of a DARPin harbors six randomized positions resulting in a theoretical diversity of 10^{23} different molecules in assembled DARPin libraries (Binz et al., 2004). These libraries

are generally used for binder selections against various different targets using ribosome display, an *in vitro* selection technique (Hanes and Plückthun, 1997). In addition, DARPins have also been successfully selected using phage display (Steiner et al., 2008).

Numerous DARPin selections yielding high affinity binders for particular target proteins have been reported (Amstutz et al., 2005; Sennhauser et al., 2007; Stefan et al., 2011). In the past, we used DARPin libraries to select highly specific inhibitors for caspase 2 (Schweizer et al., 2007) and caspase 3 (Schroeder et al., 2013) as well as binders for pro- and active caspase 7 that prevent procaspase 7 activation (Flütsch et al., 2014).

Here, we describe the general procedure for the selection of DARPin binders in parallel against the panel of human caspase 1–9. The selection led to high-affinity binders with the exception of caspase 4. Besides the previously reported specific DARPins for caspase 2 (Schweizer et al., 2007), caspase 3 (Schroeder et al., 2013), and caspase 7 (Flütsch et al., 2014), we report novel binders for caspases 1, 5, 6, 8, and 9. The binder's target specificity for caspases 1, 5, 6, and 8 was evaluated using a subset of caspase family members. In addition, we solved the first crystal structure of caspase 8 in complex with DARPin D8.4 and provide a comparison and analysis of the binding interface with the other three previously published caspases 2, 3, and 7/DARPin complex interfaces.

Results

Caspase purification

Because the targeted protein's purity and stability is crucial to prevent selection against impurities or degradation products, we have established purification protocols with high reproducibility for caspase 1–9 (Roschitzki-Voser et al., 2012). The kinetic characterization in combination with analysis of the oligomeric state determined by size exclusion chromatography (SEC) and the purity by SDS page ensured that the targeted caspases were properly folded and active enzymes.

Selection and characterization of caspase-targeted DARPins

DARPin selection was performed using ribosome display against caspases 1–9. We modified the selection protocol to achieve specificity and introduced pre-panning steps against the closest homologues of the targeted caspases in the first and third selection rounds (Supplementary Figure 1). Furthermore, additional washing has been performed to obtain a slow off rate using an excess of non-biotinylated targeted caspase after the panning step in the second and fourth rounds (Supplementary Figure 1). After four rounds of selection, the enriched caspase-targeted DARPin libraries have been used to analyze individual clones by crude extract ELISA. In general, binders that exhibited strong signal to the targeted caspases compared with the maltose-binding protein (MBP) control obtained a unique identifier (DX.Y), with X indicating the targeted caspases and Y the sequence of discovery. Obtained DARPins were sequenced (Supplementary Figure 2), purified, and analyzed for complex formation with the targeted caspase in solution using SEC (Figure 1A and Supplementary Figure 3). Notably, binding of the DARPins can occur to the monomeric as well as to the dimeric form of the targeted caspase. In addition, SEC traces suggest that binding of D1.73 and D8.4 may alter the oligomeric state of the targeted caspase. While first results using ultracentrifugation and D8.4 support these findings (data not shown), further experiments will be necessary to fully confirm an induced change of the oligomeric state upon DARPin binding.

Affinity of binders that displayed unambiguous sequencing results and a stable complex on SEC were analyzed using surface plasmon resonance (SPR) (e.g., caspase 8/D8.4 in Figure 1B). Following this approach, we were able to identify DARPins with affinities in the low nanomolar range to caspases 1–9 with the exception of caspase 4. Measured SPR data for these binders are summarized in Figure 1C, where we included the previously reported values of DARPins with high specificity for caspase 2 (Schweizer et al., 2007), caspase 3 (Schroeder et al., 2013), and pro- and active caspase 7 (Flütsch et al., 2014). Kinetic data have been obtained by fitting the measured data with the heterogeneous ligand model (Bravman et al., 2006), with exception of D9.2, which exhibited a very low signal. Different values of K_{d1} and K_{d2} can be explained by altered accessibility of the two binding epitopes most probably originating from the direct coating of the caspase molecules via biotin on the sensor chip. However, we cannot fully exclude a cooperative binding mechanism in case of the caspase 3 binders that exhibit a large difference between these two values.

In case of D8.4, the Langmuir model was used to fit the data (Figure 1B) obtaining a K_d of 5.2 nM. With the exception of D1.73, D8.1, and D8.4, which exhibited high χ^2 values while curve fitting, binding constants were determined by equilibrium analysis. DARPins that were selected against caspase 4 exhibited binding in the low
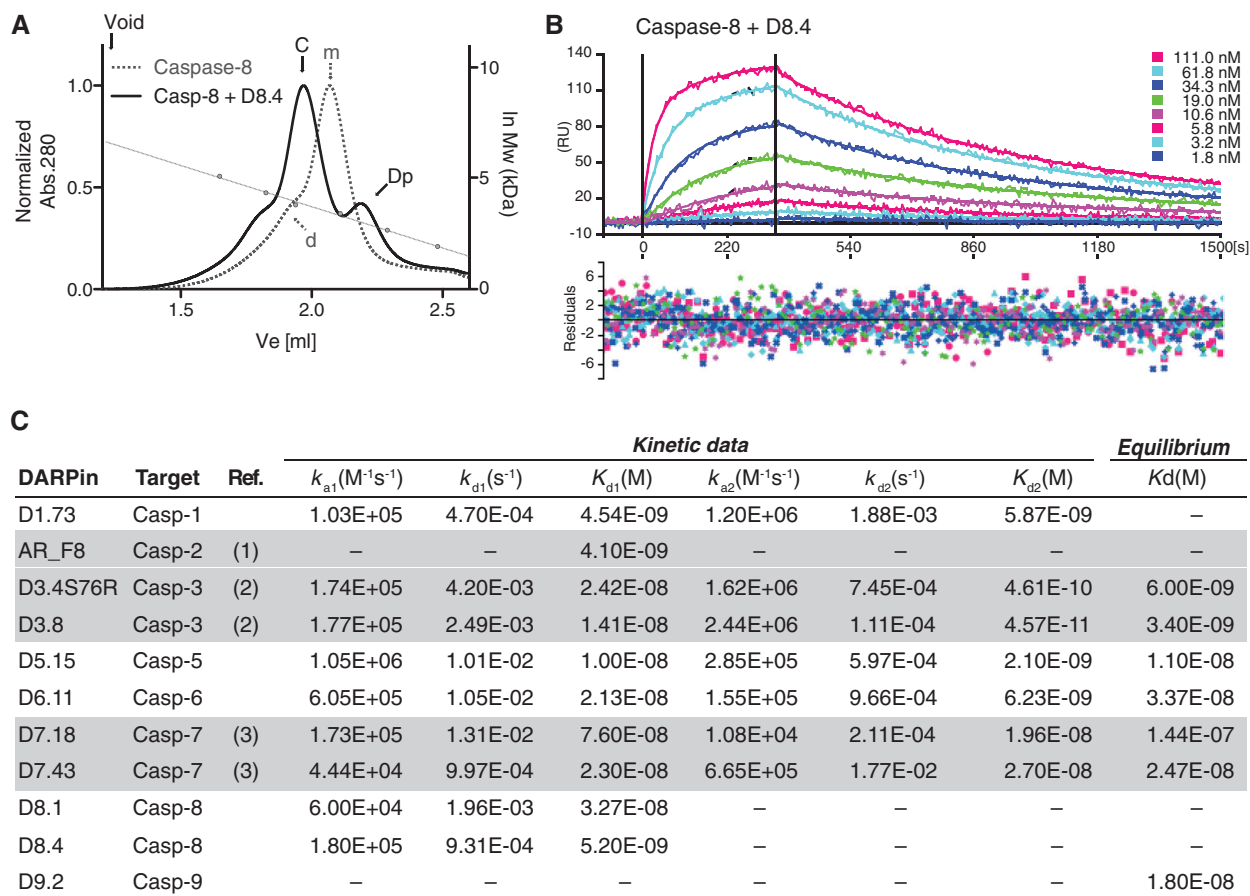
A

Void

Caspase-8
Casp-8 + D8.4

Normalized Abs.280 / ln Mw (kDa)

Ve [ml]

B Caspase-8 + D8.4

111.0 nM
61.8 nM
34.3 nM
19.0 nM
10.6 nM
5.8 nM
3.2 nM
1.8 nM

(RU)

Residuals

C

DARPin	Target	Ref.	k_{a1}(M^{-1}s^{-1})	k_{d1}(s^{-1})	K_{d1}(M)	k_{a2}(M^{-1}s^{-1})	k_{d2}(s^{-1})	K_{d2}(M)	Equilibrium Kd(M)
					Kinetic data				
D1.73	Casp-1		1.03E+05	4.70E-04	4.54E-09	1.20E+06	1.88E-03	5.87E-09	–
AR_F8	Casp-2	(1)	–	–	4.10E-09	–	–	–	–
D3.4S76R	Casp-3	(2)	1.74E+05	4.20E-03	2.42E-08	1.62E+06	7.45E-04	4.61E-10	6.00E-09
D3.8	Casp-3	(2)	1.77E+05	2.49E-03	1.41E-08	2.44E+06	1.11E-04	4.57E-11	3.40E-09
D5.15	Casp-5		1.05E+06	1.01E-02	1.00E-08	2.85E+05	5.97E-04	2.10E-09	1.10E-08
D6.11	Casp-6		6.05E+05	1.05E-02	2.13E-08	1.55E+05	9.66E-04	6.23E-09	3.37E-08
D7.18	Casp-7	(3)	1.73E+05	1.31E-02	7.60E-08	1.08E+04	2.11E-04	1.96E-08	1.44E-07
D7.43	Casp-7	(3)	4.44E+04	9.97E-04	2.30E-08	6.65E+05	1.77E-02	2.70E-08	2.47E-08
D8.1	Casp-8		6.00E+04	1.96E-03	3.27E-08	–	–	–	–
D8.4	Casp-8		1.80E+05	9.31E-04	5.20E-09	–	–	–	–
D9.2	Casp-9		–	–	–	–	–	–	1.80E-08

Figure 1 Binding characterization of selected DARPins.
(A) Selected DARPins were analyzed on SEC for the formation of a stable complex in solution (see also Supplementary Figure 3). Caspase 8 exhibits a monomer-dimer equilibrium [marked with (m) and (d), respectively]. D8.4 binds to both the monomer and the dimeric forms of caspase 8 and elutes at earlier retention volume as a protein complex (solid lines, complex peak marked with (C) and (Dp) for DARPin excess). Calibration curve (right ordinate) was made using aldolase (158 kDa), conalbumin (75 kDa), ovalbumin (43 kDa), carbonic anhydrase (29 kDa), ribonuclease A (13.7 kDa), and aprotinin (6.5 kDa). Furthermore, (B) binding affinities were determined using SPR. (C) Binding affinities and kinetic constants of selected DARPins. Binders with two indicated kinetic constants were determined using the heterogeneous ligand model (Bravman et al., 2006). D8.1 and D8.4 kinetic data were determined using the Langmuir model. The equilibrium K_D determination for D1.73, D8.1, and D8.4 resulted in high χ^2 values and are therefore excluded. Previously reported DARPins are indicated with a gray background, and references are given with numbers: (1) Schweizer et al. (2007), (2) Schroeder et al. (2013), (3) Flütsch et al. (2014).

millimolar range, three orders of magnitude higher than the best binders we have found against the other caspases. An explanation for that observation could be that caspase 4 is less stable under selection conditions. Protein sequence and biophysical properties of the DARPins listed in Figure 1C can be found in Supplementary Table 1.

Caspase specificity of the selected DARPins was determined using SPR analysis against a representative set of caspases (caspases 1, 4, 5, 6, 7, and 8) including members of all different pre-panning groups (see Supplementary Figure 1). Caspase 3 was excluded due to its lower stability when coated on the SPR chip, whereas caspases 2 and 9 were represented by the panning group member

caspase 8. Although not all caspases were tested in particular, the chosen array of different caspases is well suitable to elucidate the binder's specificity. It confirms that pre-panning during selection leads to not only specificity within a panning group (e.g., caspases 1, 4, and 5) but also across panning groups with more distantly related caspases (e.g., caspases 1, 7, and 8).

With the exception of D9.2, we tested and confirmed the binders' specificity for the targeted caspases. Caspase 8 binding specificity was tested using DARPin D8.1, which shares a very similar sequence with D8.4 with only two point mutations (Q26R and V139A, see Supplementary Figure 5) suggesting the same binding

interaction. Binding specificities for AR_F2, D3.4S76R, D3.8, D7.18, and D7.43 were reported previously (Schweizer et al., 2007; Schroeder et al., 2013; Flütsch et al., 2014).

Crystal structure of caspase 8 in complex with D8.4

To obtain a better understanding of the binding interactions between a selected DARPin and the targeted caspase, we have crystallized caspase 8 in complex with DARPin D8.4 and determined the structure at 1.8 Å resolution. Structure determination details and refinement statistics are listed in Supplementary Table 2. Crystals grew under acidic conditions at pH 4.9, indicating that the protein interaction remains intact even at low pH. This was also tested in ELISA format (data not shown) and showed that binding still occurs at acidic pH values, although a lower signal compared with neutral pH suggests a weakened binding affinity. The asymmetric unit contains a caspase 8 dimer

consisting of two small and two large subunits, two bound inhibitor molecules Ac-IETD-CHO, and two bound DARPins (Figure 2A). The binding epitope is localized on the side of the large subunit of the enzyme and primarily involves residues of α-helix α2 as well as β-strand β2 (Figure 2B).

In total, 25 caspase 8 residues are involved in binding to 31 residues of the DARPin spanning a binding interface of 938 Å². Sixteen hydrogen bonds and 7 salt bridges surround a hydrophobic core, which is formed by amino acids Phe-56, Leu-86, Leu-89, Phe-90, and Phe-123 of the DARPin and Gln-291, Ile-295, and Ile-298 of caspase 8 (Figure 2B). Remarkably, besides the 16 non-randomized residues that are involved in binding, D8.4 possesses two unintended framework mutations (Arg-26 and Arg-85, see Supplementary Figure 5), which play a role in hydrogen bonding to caspase 8 (marked in Figure 2B, left).

As intended, the specificity of D8.4 for caspase 8 is achieved by targeting of non-conserved residues. Especially the hydrophobic interaction provided by Ile-298
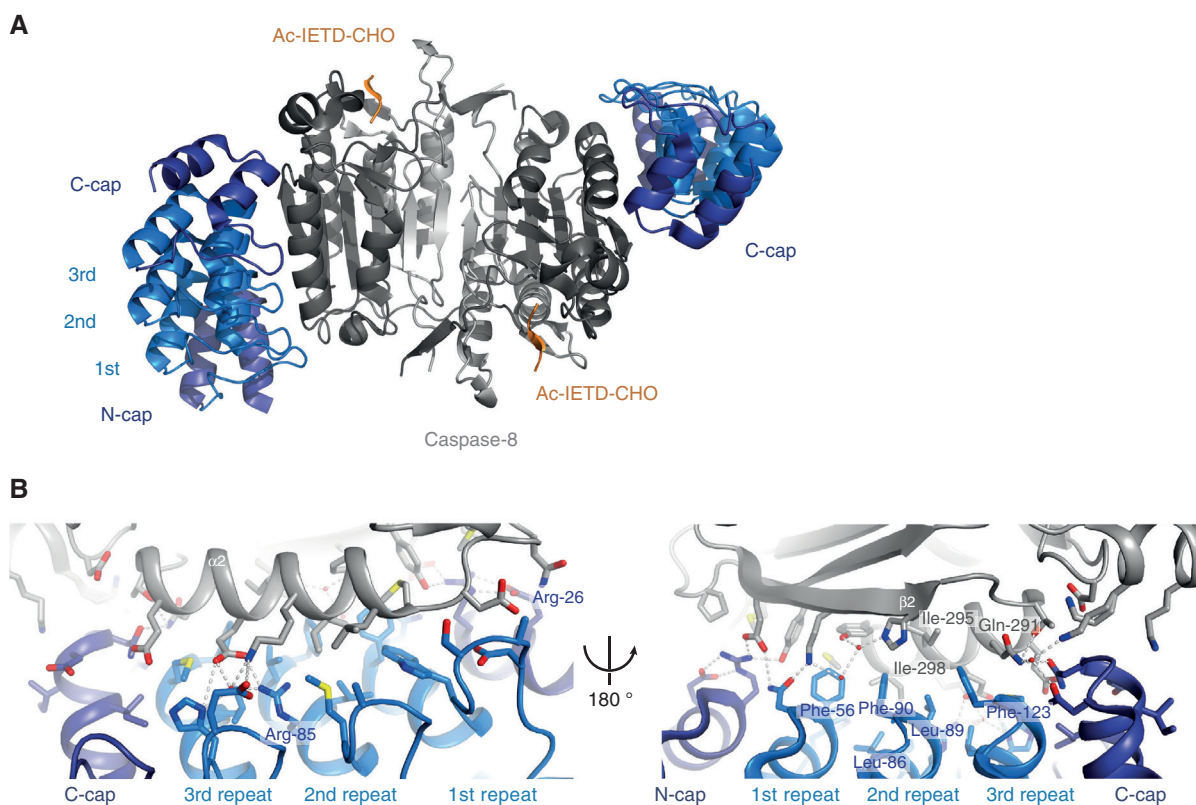

Figure 2 Caspase 8 in complex with DARPin D8.4.
(A) Standard view of caspase 8 (small subunit in light gray, large subunit in dark gray, Ac-IETD-CHO inhibitor in orange) in complex with DARPin D8.4 (N- and C-cap in dark blue, internal repeats are light blue). The DARPin binds lateral at the large subunit of the enzyme. (B) Close-up view of the caspase 8/DARPin D8.4 binding interface displaying the major interactions between the DARPin and α-helix α2 of caspase 8 (left) and the interactions of D8.4 with β-strand β2 of caspase 8 (right). Important residues are labeled in blue (DARPin) and gray (caspase 8). See also Supplementary Figure 5 for a list of interacting residues.

(Figure 2B, right) is not conserved among the apoptotic caspases, which harbor a larger and more hydrophilic residue at this position (Supplementary Figure 5). Besides that, only Thr-288 at the beginning of α-helix α1 was identified as highly conserved. Therefore, our crystal structure not only provides insights into the binding interface but also elucidates the specificity of the selected DARPin. In addition, it confirms our chosen selection procedure with the additional pre-panning steps against homologues caspases. A structural alignment of our caspase 8/DARPin-8.4 structure with the high-resolution structure of the same enzyme (1QTN; Watt et al., 1999) results in a very low root mean square deviation of about 0.7 Å, indicating no or only minor differences between the two structures. While they show no structural differences in the overall fold and the active site, several side chains in the caspase/DARPin interface adopt different conformations (e.g., Glu-290, Glu-294, Ile-298) due to the presence of the DARPin D8.4.

DARPin binding interfaces on human caspases

With the previously described crystal structures of caspases in complex with specific DARPins (Schweizer et al., 2007; Schroeder et al., 2013; Flütsch et al., 2014), we were able to compare the different DARPin epitopes for each particular caspase (Figure 3).

Based on the caspase standard view, where the five main parallel β-strands (β1–β5) of a caspase protomer are aligned with their C-termini pointing upwards, caspase 2-specific DARPin AR_F8 (Figure 3A; Schweizer et al., 2007) binds apical at the backside of loop 4 (also known as loop 381; Fuentes-Prior and Salvesen, 2004), which is involved in the formation of the active site cleft. Because this loop is not highly conserved among other caspases, it explains the high specificity of DARPin AR_F8 for caspase 2. The binding area of 799 Å^2 includes a hydrophobic core, six hydrogen bonds, and nine salt bridges. AR_F8 binding at the backside of loop 4 leads to a loop shift of 1 Å and opens the active site cleft (Schweizer et al., 2007). This finally results in a displacement of the active site cysteine (Cys-155) and structurally elucidates the allosteric mode of inhibition.

Although DARPin D3.4S76R binds in a similar way apical to caspase 3 (Figure 3B; Schroeder et al., 2013) at the active site forming loops, the epitope is only partially overlapping with that of caspases 2 and AR_F8. D3.4S76R binds directly into the active site pocket of caspases 3 and only interacts with the tip of loop 4. Its high specificity is achieved by the formation of a salt bridge between Lys-56

and the Asp-253 of caspase 3. Interestingly, the interacting DARPin residue Asp-45 occupies the S4 pocket of the enzyme, as it can be observed in binding of peptide substrates. In addition, Ile-78 of the DARPin keeps Tyr-204 of caspase 3 in a conformation that blocks the S2 binding pocket. Overall, the binding of D3.4S76R to caspase 3 prevents substrate entrance to the active site pocket and mimics an interaction seen for caspase 3 with its natural inhibitor XIAP (Schroeder et al., 2013). Enzyme kinetic analysis has classified D3.4S76R as a purely competitive inhibitor.

Besides the apical binding sites of AR_F8 and D3.4S76R, another favored caspase/DARPin epitope could be identified laterally at the large subunit of the peptidase. In addition to the above-described DARPin D8.4 that binds sideways at the large subunit (p20) primarily to residues of α-helix α2 (Figure 3D), DARPins that have been selected against caspase 7 bind at a similar epitope (Flütsch et al., 2014). For instance, the crystal structure of caspase 7 in complex with DARPin D7.18 (Figure 3C) unraveled a binding interface of 672 Å^2 that is predominantly formed by residues located on β-strand β2. In particular, two DARPin tryptophans (Trp-46 and Trp-78) are deeply buried in a hydrophobic pocket shaped by non-conserved residues of caspase 7. Because this hydrophobic pocket is obstructed in other homologues, these two tryptophans are the major contributors for the high specificity of DARPin D7.18. Although there is another caspase 7/DARPin complex structure available (pdb: 4JB8; Seeger et al., 2013) with DARPin C7_16 binding laterally at the large subunit of caspases 7, we excluded this protein complex in our structural analysis. This DARPin has been selected without additional pre-panning steps and thus may lack specificity.

More interestingly, D7.43 and D7.18 also bind to pro caspase 7, thus preventing a successful activation (Flütsch et al., 2014). D8.4 with a lateral but different binding epitope would suggest a potential effect on the activation mechanism in analogy to the caspase 7 DARPins. However, the activation mechanism of caspase 8 is different compared with the caspase-mediated cleavage of procaspase 7. It occurs via autocatalytic processing after proximity-induced oligomerization (Salvesen and Dixit, 1999) and therefore is dependent on the oligomeric state of caspase 8. Complex formation on SEC (Figure 1A) and first ultracentrifugation experiments (data not shown) demonstrate that D8.4 can bind to the monomer as well as to the dimer of caspase 8 *in vitro*. Whether binding in a cellular environment to the full procaspase 8 with its two N-terminal death effector domains occurs and modulates caspase 8 activation has not been further analyzed and remains unknown.

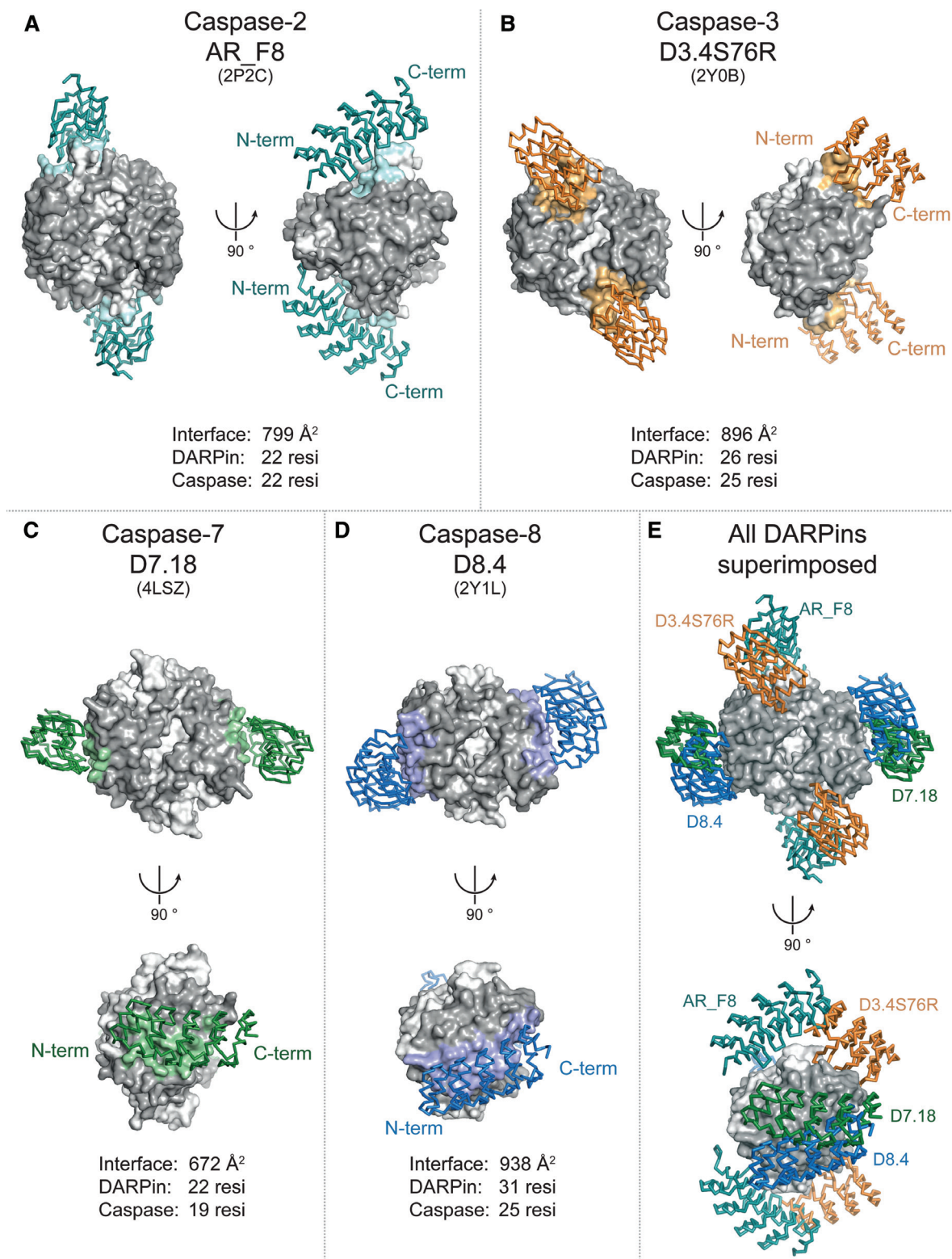All the complex structures display binding of one selected DARPin to one caspase protomer; thus, every

A Caspase-2
AR_F8
(2P2C)

Interface: 799 Å^2
DARPin: 22 resi
Caspase: 22 resi

B Caspase-3
D3.4S76R
(2Y0B)

Interface: 896 Å^2
DARPin: 26 resi
Caspase: 25 resi

C Caspase-7
D7.18
(4LSZ)

Interface: 672 Å^2
DARPin: 22 resi
Caspase: 19 resi

D Caspase-8
D8.4
(2Y1L)

Interface: 938 Å^2
DARPin: 31 resi
Caspase: 25 resi

E All DARPins
superimposed

Figure 3 Caspase-specific DARPins: complex structure overview.
Currently available caspase structures in complex with specific DARPins are shown in standard view and rotated (90° around the y-axes).
Interacting residues on the caspase surface are colored according to the color of the binding DARPin. (A) AR_F8 binds caspase 2 from the
backside of loop 4. (B) D3.4S76R blocks the active site cleft of caspase 3. (C) D7.18 binds at the large subunit (p20) of caspase 7. (D) A
similar epitope can be observed for caspase 8-specific DARPin D8.4. (E) Superposition of all DARPins on caspase 8 visualizes the different
epitopes. See also Supplementary Figure 6 for a sequence alignment of all caspases and the interacting caspase residues.

caspase dimer has two DARPins bound. A superposition of all DARPins on caspase 8 shows the particular difference between the binding interfaces and emphasizes similarities (Figure 3E). While the apical epitope of DARPin AR_F8 is located at the backside of loop 4, D3.4S76R binds inside the active site cleft and completely blocks an entrance of substrate. The lateral binding at the large subunit is less distinct. DARPin D7.18 and D8.4 share a similar binding area on the caspase surface, but their position is slightly tilted by an angle of 30°. Notably, the N-terminus of all DARPins is oriented to the backside in the standard caspase representation resulting in a 'dorsal to ventral' DARPin orientation.

Comparison of these DARPin epitopes on the caspase surface suggests that binding in specific manner is more likely if it occurred at the outer rim of the enzyme rather than centrally located close to the dimer interface of two caspase protomers. However, we cannot exclude that this finding is experimentally influenced by the immobilization of the caspase molecule during the selection procedure. Random chemical biotinylation may orient the enzyme in a particular direction that binding to the outer rim is more likely. Besides that, it has been shown that the central cavity formed by two caspase protomers is conserved between caspases 3 and 7 (Hardy et al., 2004), suggesting a less favored epitope for high caspase specificity in close proximity to the cavity. In addition, exosite studies on caspase 7 revealed that surface residues located at the large subunit influence the cleavage efficiency for particular substrates (Boucher et al., 2012). For example, a caspase 7 mutant (K69L) exhibited reduced processing of the Hsp90 co-chaperone p23. More interestingly, Lys-69 is also involved in binding to DARPin D7.18, is not conserved in other caspases (see Supplementary Figure 6) and the caspase 8 homologue residue (Tyr-235) also contributes to DARPin D8.4 binding. Although very preliminary, this finding indicates that the non-conserved caspase residues involved in DARPin binding might also be of importance in providing specific binding interactions to certain caspase substrates.

Discussion

Using the here-described DARPin selection procedure including pre-panning steps against close homologues, we obtained new binders against five members of the human caspase family. We characterized these novel DARPins for caspases 1, 5, 6, 8, and 9 and included data of the previously reported specific binders for caspases 2, 3, and 7 (Schweizer et al., 2007; Schroeder et al., 2013; Flütsch et al., 2014). Caspase specificity of the new DARPins D1.73,

D5.15, D.6.11, and D8.1 was tested using a subset of caspase family members (caspases 1, 4, 5, 6, 7, and 8). Although our results suggest high target specificity, binding of the DARPins to caspases 2, 3, and 9 was not tested.

The crystal structure of caspase 8 in complex with DARPin D8.4 provides insights into the binding mode of this high affine binder. D8.4 binds lateral to the p20 subunit of the enzyme and does not interfere with the active site of the enzyme. The binding interface of caspase 8 involves a hydrophobic patch consisting of several non-conserved caspase residues and thus explains its specificity. Although the previously reported DARPins for caspases 2, 3, and 7 are binders with inhibitory function (Schweizer et al., 2007; Schroeder et al., 2013; Flütsch et al., 2014), the here newly reported DARPins do not prevent cleavage of small peptide substrates *in vitro*. If these binders can interact with the targeted procaspases and interfere with the activation process has not been tested and needs to be addressed in future experiments.

A structural comparison of all available caspase/ DARPin complexes reveals two distinct binding regions on the caspase surface. One is located apical close or at the active site. Here the DARPins interact with active site forming loops or with residues in the active site and thereby inhibit the enzyme either allosterically or competitively. The other favored region is found laterally at the large subunit of the peptidase and involves α-helix α1 and α2 as well as β-strand β2. With this study, we show that specific DARPins can be selected against a particular member of a highly homologous protein family sharing a high sequence identity. Thus, these DARPins provide a molecular toolbox for functional and structural investigations either *in vitro* or in cell-based assays using mammalian expression vectors.

Materials and methods

All reagents were bought from Sigma/Fluka if not stated otherwise. Sequencing was performed at Microsynth (Balgach, Switzerland).

Caspase purification and biotinylation

Caspase 1–9 have been purified as described previously (Roschitzki-Voser et al., 2012). Ribosome display selection and ELISA experiments were performed using chemically biotinylated caspases (EZ-Link Sulfo-NHS-LC-LC-Biotin, 21338; Pierce Biotechnology, Rockford, IL, USA). After purification, 1 ml of caspase (10 μM) in phosphate buffer saline (PBS), pH 7.3, or 50 mM HEPES, pH 7.5, containing 150 mM NaCl was incubated with a molar excess (7×, 70 μM) of biotin on ice for 30 min. The reaction was quenched by adding 5 M Tris pH 7.5 (10 μl). Biotinylated proteins were purified by SEC using a Superdex 200 10/300 GL (GE Healthcare, Piscataway,

NJ, USA) equilibrated in PBS at 4°C. Fractions containing biotinylated caspases were pooled, frozen in liquid nitrogen after adding sucrose (10%), and stored at -80°C in small aliquots.

DARPin selection by ribosome display

Cloning and amplification of a DARPin library has been described previously (Binz et al., 2003) and a library containing NI3C and NI2C DARPins was used for selections by ribosome display (Hanes and Plückthun, 1997; Zahnd et al., 2007). The selection procedure was slightly modified with focus on specificity and low k_{off} rates (see Supplementary Figure 1). To prevent unspecific binding to random proteins, each round included a pre-panning step for MBP (coated 22 nM). In addition, two of the most homologues caspases were included in pre-panning steps (coated 22 nM) in rounds 1 and 3. k_{off} maturation was done by adding a 100- and 500-fold excess of unbiotinylated caspase for 5 or 10 min in rounds 2 and 4, respectively. Unbound DARPin/ribosome complexes were washed after each round with increasing stringency (Supplementary Figure 1). The enriched library was cloned after 4 selection rounds into a pQE30 vector and transfected to XL1-Blue *Escherichia coli* cells (Stratagene, La Jolla, CA, USA).

Crude extract ELISA

Single *E. coli* colonies, each expressing one selected DARPins, were picked and inoculated in 900 µl auto-inducing media (Studier, 2005) using 96-well plates (Abgene by Fisher Scientific, Wohlen, Switzerland). Cells grew over night at 37°C; 200 µl of each well were then transferred to a 96-well plate (Nunc by Thermo Fisher Scientific, Waltham, MA, USA) for plasmid preparation, and 700 µl were harvested by centrifugation. Cells were lysed using B-PER II (50 µl, 78260; Pierce Biotechnology, Rockford, IL, USA) per well (30 min, shaking at room temperature). Lysis buffer was neutralized with PBS (950 µl) and cell debris was removed by centrifugation (20 min, 4500 rpm at 4°C). A 20-µl supernatant were transferred to 384 well ELISA plates (Nunc by Thermo Fisher Scientific, Waltham, MA, USA), which were prepared in advance with either immobilized MBP or targeted caspase. For immobilization, plates were coated using NeutrAvidin solution (20 µl at 22 nM, 31000; Pierce Biotechnology, Rockford, IL, USA), followed by incubation of biotinylated proteins and extensive washing. Cell lysate supernatants containing the expressed DARPin were incubated for 1 h at room temperature. After three washing cycles (PBS), each well was incubated with mouse anti-RGS-H4 antibody (1:2000 in PBS+1% bovine serum albumin, 34650; Qiagen, Boston, MA, USA). After washing, the secondary antibody (goat α-mouse IgG alkaline phosphatase conjugate from Sigma; A3562) was incubated. After four washing cycles, the substrate (3 mM di-sodium 4-nitrophenyl phosphate in 50 mM $NaHCO_3$, 50 mM $MgCl_2$) was added and $OD_{405\,nm}$ was measured using a multiwell plate reader (Tecan Infinity M1000, Tecan, Männedorf, Switzerland). DARPins exhibited strong signals (>5-fold vs. MBP control) were sequenced.

Expression and purification of DARPins

DARPins were expressed in auto-inducing media (Studier, 2005) overnight or in 2YT (3 h at 37°C) after the induction with isopropyl β-D-1-thiogalactopyranoside (0.5 mM, IPTG) at an $OD_{600\,nm}$ between 0.6 and 1. Cells were harvested (6000 rpm, 5 min, 4°C; Biofuge primo R, Heraeus, Hanau, Germany) and lysed by ultrasonification. DARPin purification was performed by immobilized metal-affinity chromatography (gravity columns, 0.5 ml Ni^{2+}-NTA agarose beads, 30210; Qiagen, Boston, MA, USA). DARPins were eluted in PBS, 200 mM imidazole, pH 7.4. Imidazole was removed using a PD-10 desalting column (17-0435-01; GE Healthcare, Piscataway, NJ, USA). For storage at 4°C, 0.05% sodium azide (NaN_3) was added, whereas 20% glycerol was used for storage at -20°C.

Complex formation on SEC

Purified caspases were incubated with a 2-fold molar excess of selected DARPins. Protein solutions were applied on SEC using a Superdex 200 5/150 GL column (GE Healthcare, Piscataway, NJ, USA) equilibrated in 50 mM Tris, 150 mM NaCl, pH 7.5. Absorption at 280 nm was recorded and analyzed in Prism (Version 5, GraphPad Software, La Jolla, CA, USA).

SPR analysis

SPR experiments were performed using a Proteon XPR36 (Bio-Rad Laboratories, Hercules, CA, USA) and an NLC sensor chip. Sterile filtered PBS, pH 7.3, 0.005% Tween 20, was the standard buffer for all coating and kinetic measurements. Approximately 1000 RU of biotinylated caspases (5 nM) were coated on the chip at 30 µl/min. Dilution series of DARPin analytes were prepared prior to the experiment in 96-well plates and sealed to prevent evaporation or contamination. At least eight different concentrations (0–500 nM) starting with the lowest concentration were measured at 20°C. Due to the heterogeneity of the system, the chip surface was not regenerated between different analyte concentration but dissociation time could be prolonged up to 30 min. In general, experiments were performed at flow rates of 100 µl/min with 5-min association phases and 20 min dissociation phases. Recorded data were processed and evaluated using ProteOn Manager 2.1.1 (Bio-Rad Laboratories, Hercules, CA, USA). Binding kinetics and affinities were determined by equilibrium analysis or curve fitting (Bravman et al., 2006).

Crystallization of caspase 8 in complex with DARPin D8.4

Caspase 8 was incubated with a 2-fold molar excess of DARPin D8.4 (10 min on ice). The formed complex was separated using a Superdex 200 10/300 GL column (GE Healthcare, Piscataway, NJ, USA), 20 mM Tris, pH 7.5 (4°C), 20 mM NaCl. Fractions containing the dimeric caspase 8/D8.4 complex were pooled and concentrated (15–21 mg/ml) using an Amicon Ultra centrifugation device (10 kDa MWCO, EMD Milipore, Darmstadt, Germany). Prior to crystallization, the protein solution was incubated with a peptide aldehyde inhibitor Ac-IETD-CHO (two inhibitors per active site). Crystals were grown at room temperature using sitting-drop vapor-diffusion method (100 mM citric acid, pH 4.9, 200 mM Li_2SO_4, and 22.4% PEG 4000). For cryoprotection, the

crystals were equilibrated in reservoir buffer containing ethylene glycol (10%–15%) and flash frozen in a nitrogen stream at -170°C.

X-ray diffraction, data collection, and structure determination

Diffraction data were collected at the Swiss Light Source (SLS, X06SA beamline) on a Pilatus 6M fast readout pixel detector. XDS (Kabsch, 2010) was used for data processing. The crystal structure was solved by molecular replacement using PHASER (McCoy et al., 2007) and the structure of caspase 8 (1QDU) (Blanchard et al., 1999) and a NI3C-DARPin (2QYJ) (Merz et al., 2008) as search model. Structure refinement was performed with REFMAC 5.5.01.09 (Murshudov et al., 1997) and binding interface analysis was done using the EPPIC server (Duarte et al., 2012) (www.eppic-web.org). Structure figures were prepared in PyMOL (http://www.pymol.org).

Accession numbers

Atomic coordinates and structure factors of caspase 8/D8.4 were deposited in the Protein Data Bank (2Y1L).

Competing financial interests

T.S. is partner at Nextech Invest Ltd. and R.A. is employed at Cilag AG. The other authors declare no competing financial interest.

References

Amstutz, P., Binz, H.K., Parizek, P., Stumpp, M.T., Kohl, A., Grütter, M.G., Forrer, P., and Plückthun, A. (2005). Intracellular kinase inhibitors selected from combinatorial libraries of designed ankyrin repeat proteins. J. Biol. Chem. *280*, 24715–24722.

Binz, H.K., Stumpp, M.T., Forrer, P., Amstutz, P., and Plückthun, A. (2003). Designing repeat proteins: well-expressed, soluble and stable proteins from combinatorial libraries of consensus ankyrin repeat proteins. J. Mol. Biol. *332*, 489–503.

Binz, H.K., Amstutz, P., Kohl, A., Stumpp, M.T., Briand, C., Forrer, P., Grütter, M.G., and Plückthun, A. (2004). High-affinity binders selected from designed ankyrin repeat protein libraries. Nat. Biotechnol. *22*, 575–582.

Blanchard, H., Kodandapani, L., Mittl, P.R., Marco, S.D., Krebs, J.F., Wu, J.C., Tomaselli, K.J., and Grütter, M.G. (1999). The three-dimensional structure of caspase-8: an initiator enzyme in apoptosis. Structure *7*, 1125–1133.

Boucher, D., Blais, V., and Denault, J.B. (2012). Caspase-7 uses an exosite to promote poly(ADP ribose) polymerase 1 proteolysis. Proc. Natl. Acad. Sci. USA *109*, 5669–5674.

Bravman, T., Bronner, V., Lavie, K., Notcovich, A., Papalia, G.A., and Myszka, D.G. (2006). Exploring "one-shot" kinetics and small molecule analysis using the ProteOn XPR36 array biosensor. Anal. Biochem. *358*, 281–288.

Duarte, J.M., Srebniak, A., Schärer, M.A., and Capitani, G. (2012). Protein interface classification by evolutionary analysis. BMC Bioinform. *13*, 334.

Favaloro, B., Allocati, N., Graziano, V., Di Ilio, C., and De Laurenzi, V. (2012). Role of apoptosis in disease. Aging *4*, 330–349.

Flütsch, A., Ackermann, R., Schroeder, T., Lukarska, M., Hausammann, G.J., Weinert, C., Briand, C., and Grütter, M.G. (2014). Combined inhibition of caspase 3 and caspase 7 by two highly selective DARPins slows down cellular demise. Biochem. J. *461*, 279–290.

Fuentes-Prior, P. and Salvesen, G.S. (2004). The protein structures that shape caspase activity, specificity, activation and inhibition. Biochem. J. *384*, 201–232.

Grütter, M.G. (2000). Caspases: key players in programmed cell death. Curr. Opin. Struct. Biol. *10*, 649–655.

Hanes, J. and Plückthun, A. (1997). In vitro selection and evolution of functional proteins by using ribosome display. Proc. Natl. Acad. Sci. USA *94*, 4937–4942.

Hardy, J.A., Lam, J., Nguyen, J.T., O'Brien, T., and Wells, J.A. (2004). Discovery of an allosteric site in the caspases. Proc. Natl. Acad. Sci. USA *101*, 12461–12466.

Kabsch, W. (2010). Integration, scaling, space-group assignment and post-refinement. Acta Crystallogr. D Biol. Crystallogr. *66*, 133–144.

McCoy, A.J., Grosse-Kunstleve, R.W., Adams, P.D., Winn, M.D., Storoni, L.C., and Read, R.J. (2007). Phaser crystallographic software. J. Appl. Crystallogr. *40*, 658–674.

McStay, G.P., Salvesen, G.S., and Green, D.R. (2008). Overlapping cleavage motif selectivity of caspases: implications for analysis of apoptotic pathways. Cell Death Differ. *15*, 322–331.

Merz, T., Wetzel, S.K., Firbank, S., Plückthun, A., Grütter, M.G., and Mittl, P.R. (2008). Stabilizing ionic interactions in a full-consensus ankyrin repeat protein. J. Mol. Biol. *376*, 232–240.

Murshudov, G.N., Vagin, A.A., and Dodson, E.J. (1997). Refinement of macromolecular structures by the maximum-likelihood method. Acta Crystallogr. D Biol. Crystallogr. *53*, 240–255.

Rohn, T.T. (2010). The role of caspases in Alzheimer's disease; potential novel therapeutic opportunities. Apoptosis *15*, 1403–1409.

Roschitzki-Voser, H., Schroeder, T., Lenherr, E.D., Frölich, F., Schweizer, A., Donepudi, M., Ganesan, R., Mittl, P.R., Baici, A., and Grütter, M.G. (2012). Human caspases in vitro: expression, purification and kinetic characterization. Protein Expr. Purif. *84*, 236–246.

Salvesen, G.S. and Dixit, V.M. (1999). Caspase activation: the induced-proximity model. Proc. Natl. Acad. Sci. USA *96*, 10964–10967.

Schroeder, T., Barandun, J., Flütsch, A., Briand, C., Mittl, P.R., and Grütter, M.G. (2013). Specific inhibition of caspase-3 by a competitive DARPin: molecular mimicry between native and designed inhibitors. Structure *21*, 277–289.

Schweizer, A., Roschitzki-Voser, H., Amstutz, P., Briand, C., Gulotti-Georgieva, M., Prenosil, E., Binz, H.K., Capitani, G., Baici, A., Plückthun, A., et al. (2007). Inhibition of caspase-2 by a designed ankyrin repeat protein: specificity, structure, and inhibition mechanism. Structure *15*, 625–636.

Seeger, M.A., Zbinden, R., Flütsch, A., Gutte, P.G., Engeler, S., Roschitzki-Voser, H., and Grütter, M.G. (2013). Design, construction, and characterization of a second-generation DARPin library with reduced hydrophobicity. Protein Sci. *22*, 1239–1257.

Sennhauser, G., Amstutz, P., Briand, C., Storchenegger, O., and Grütter, M.G. (2007). Drug export pathway of multidrug exporter AcrB revealed by DARPin inhibitors. PLoS Biol. *5*, e7.

Stefan, N., Martin-Killias, P., Wyss-Stoeckle, S., Honegger, A., Zangemeister-Wittke, U., and Plückthun, A. (2011). DARPins recognizing the tumor-associated antigen EpCAM selected by phage and ribosome display and engineered for multivalency. J. Mol. Biol. *413*, 826–843.

Steiner, D., Forrer, P., and Plückthun, A. (2008). Efficient selection of DARPins with sub-nanomolar affinities using SRP phage display. J. Mol. Biol. *382*, 1211–1227.

Studier, F.W. (2005). Protein production by auto-induction in high density shaking cultures. Protein Expr. Purif. *41*, 207–234.

Taylor, R.C., Cullen, S.P., and Martin, S.J. (2008). Apoptosis: controlled demolition at the cellular level. Nat. Rev. Mol. Cell Biol. *9*, 231–241.

Watt, W., Koeplinger, K.A., Mildner, A.M., Heinrikson, R.L., Tomasselli, A.G., and Watenpaugh, K.D. (1999). The atomic-resolution structure of human caspase-8, a key activator of apoptosis. Structure *7*, 1135–1143.

Zahnd, C., Amstutz, P., and Plückthun, A. (2007). Ribosome display: selecting and evolving proteins *in vitro* that specifically bind to a target. Nat. Methods *4*, 269–279.

———